Boundary Value Problems
a SpringerOpen Journal

RESEARCH Open Access

Thermodiffusion effects on magneto-nanofluid flow over a stretching sheet

Faiz G Awad, Precious Sibanda* and Ahmed A Khidir

*Correspondence:
sibandap@ukzn.ac.za
School of Mathematics, Statistics and Computer Science, University of KwaZulu-Natal, Private Bag X01, Scottsville, Pietermaritzburg, 3209, South Africa

Abstract

We study the effect of thermophoresis on boundary layer magneto-nanofluid flow over a stretching sheet. The model includes the effects of Brownian motion and cross-diffusion effects. The governing partial differential equations are transformed to a system of ordinary differential equations and solved numerically using a spectral linearisation method. The effects of the magnetic influence number, the Prandtl number, Lewis number, the Brownian motion parameter, thermophoresis parameter, the modified Dufour parameter and the Dufour-solutal Lewis number on the fluid properties as well as on the heat, regular and nano mass transfer coefficients are determined and shown graphically.

1 Introduction

Most common fluids such as water, ethylene, glycol, toluene or oil generally have poor heat transfer characteristics owing to their low thermal conductivity. A recent technique to improve the thermal conductivity of these fluids is to suspend nano-sized metallic particles such as aluminum, titanium, gold, copper, iron or their oxides in the fluid to enhance its thermal properties, Choi [1]. The enhancement of thermal conductivity in nanofluids has been studied by, among others, Kakac and Pramuanjaroenkij [2], Choi *et al.* [3], Masuda *et al.* [4], Eapen *et al.* [5] and Fan and Wang [6]. Nield and Kuznetsov [7] analyzed the behaviour of boundary layer flow on the Chen-Minkowycz problem in a porous layer saturated with a nanofluid. Nield and Kuznetsov [8] investigated thermal instability in a porous medium saturated with nanofluid using the Brinkman model. The model incorporated the effects of Brownian motion and thermophoresis of nanoparticles. They found that the critical thermal Rayleigh number can be reduced or increased by a substantial amount depending on whether the nanoparticle distribution is top-heavy or bottom-heavy. Aziz *et al.* [9] studied steady boundary layer flow past a horizontal flat plate embedded in a porous medium filled with a water-based nanofluid containing gyrotactic microorganisms. Cheng [10] investigated the behaviour of boundary layer flow over a horizontal cylinder of elliptic cross section in a porous medium saturated with a nanofluid. Chamkha *et al.* [11] investigated the non-similar solutions for natural convective boundary layer flow over a sphere embedded in a porous medium saturated with a nanofluid.

During the last few decades, fluid flow over a stretching surface has received considerable attention because of its engineering applications such as in melt-spinning, hot

rolling, wire drawing, glass-fiber production and the manufacture of polymer and rubber sheets, Altan and Gegel [12], Fisher [13], and Tidmore and Klein [14]. Nanofluid flow over a stretching surface has been investigated by many researchers. The first study on a stretching sheet in nanofluids was published by Khan and Pop [15]. Makinde and Aziz [16] performed a numerical study of boundary layer flow over a linear stretching sheet. Both Brownian motion and thermophoresis effects on the transport equations were presented. They reported that stronger Brownian motion and thermophoresis lead to an increase in the rate of heat transfer. However, the opposite was observed in the case of the rate of mass transfer. Recent studies in this area include those of Narayana and Sibanda [17] and Kameswaran *et al.* [18].

Magnetic nanofluids have numerous uses or potential applications in engineering and medicine. Using magnetic nanofluids has the potential to regulate the flow rate and heat transfer by controlling the thermo-magnetic convection current and the fluid velocity (see Shima *et al.* [19], Ganguly *et al.* [20]). The effects of a magnetic field on nanofluid flow over a stretching sheet have been investigated by, among others, Bachok *et al.* [21] and Hanad and Ferdows [22].

The aim of this study is to analyse Dufour and Soret effects in a magneto-nanofluid flow over a stretching sheet. In addition, we study Brownian motion and thermophoresis effects using a spectral linearisation method to obtain numerical solutions of the momentum, energy, concentration and mass fraction equations. The successive linearisation method (SLM) is an accurate method for solving non-linear coupled equations (see [23–25]). Recent studies such as [26–28] have suggested that the SLM is accurate and converges rapidly to the numerical results when compared to other semi-analytical methods such as the Adomian decomposition method, the variational iteration method and the homotopy perturbation method.

2 Mathematical formulation

Consider two-dimensional nanofluid flow over a linearly stretching sheet with velocity $u_w = ax$, where a is a real positive number. The coordinate system is assumed to define the x-axis along the surface of the sheet and y is the coordinate normal to the surface of the sheet. The surface temperature T_w and nanoparticle concentration $\hat{\phi}_w$ are higher than the ambient values T_∞ and $\hat{\phi}_\infty$, respectively. The governing equations for the problem can be written in the form

$$\frac{\partial u}{\partial x} + \frac{\partial v}{\partial y} = 0, \tag{1}$$

$$u\frac{\partial u}{\partial x} + v\frac{\partial u}{\partial u} + \sigma B_0^2 u = \nu\frac{\partial^2 u}{\partial y^2}, \tag{2}$$

$$u\frac{\partial T}{\partial x} + v\frac{\partial T}{\partial y} = \alpha_m\frac{\partial^2 T}{\partial y^2} + \tau\left[D_B\frac{\partial \hat{\phi}}{\partial \hat{y}}\frac{\partial T}{\partial \hat{y}} + \frac{D_T}{T_\infty}\left(\frac{\partial T}{\partial y}\right)^2\right] D_{TC}\frac{\partial^2 C}{\partial y^2}, \tag{3}$$

$$u\frac{\partial C}{\partial x} + v\frac{\partial C}{\partial y} = D_S\frac{\partial^2 C}{\partial y^2} + D_{CT}\frac{\partial^2 T}{\partial y^2}, \tag{4}$$

$$u\frac{\partial \hat{\phi}}{\partial x} + v\frac{\partial \hat{\phi}}{\partial y} = D_B\frac{\partial^2 \hat{\phi}}{\partial y^2} + \left(\frac{D_T}{T_\infty}\right)\frac{\partial^2 T}{\partial y^2}, \tag{5}$$

with the boundary conditions

$$\begin{aligned} &v = 0, \qquad u = u_w(= ax), \qquad T = T_w, \qquad C = C_w \quad \text{and} \quad \hat{\phi} = \hat{\phi}_w \quad \text{on } y = 0, \\ &u \to 0, \qquad T \to T_\infty, \qquad C \to C_\infty \quad \text{and} \quad \hat{\phi} \to \hat{\phi}_\infty \quad \text{when } \hat{y} \to \infty, \end{aligned} \tag{6}$$

where u and v are the velocity components along the x and y direction respectively, σ is the electrical conductivity, B_0 is magnetic field flux density, ν kinematic viscosity of the base fluid, α is the thermal diffusivity of the porous medium, D_B is the Brownian diffusion coefficient, D_T is thermophoresis diffusion coefficient, D_{CT} and D_{TC} are the Soret and Dufour diffusivities, D_S is the solutal diffusivity, T is the fluid temperature, C is the solutal concentration, $\hat{\phi}$ is the nanoparticle volume fraction, $(\rho c)_f$ and $(\rho c)_p$ are the heat capacity of the fluid and the effective heat capacity of the nanoparticle material respectively, τ is a parameter defined by $(\rho c)_f/(\rho c)_P$. Using the similarity variables

$$\begin{aligned} &\eta = y\sqrt{\frac{a}{\nu}}, \qquad \psi = (a\nu)^{\frac{1}{2}} f(\eta), \qquad \theta(\eta) = \frac{T - T_\infty}{T_w - T_\infty}, \\ &S(\eta) = \frac{C - C_\infty}{C_w - C_\infty}, \qquad \phi(\eta) = \frac{\hat{\phi} - \hat{\phi}_\infty}{\hat{\phi}_w - \hat{\phi}_\infty}, \end{aligned} \tag{7}$$

equations (1)-(5) reduce to the following non-similar forms where primes denote differentiation with respect to η:

$$f''' + ff'' - f'^2 - Mf' = 0, \tag{8}$$

$$\theta'' + Prf\theta' + PrNb\theta'\phi' + PrNt\theta'^2 + NdS'' = 0, \tag{9}$$

$$S'' + LefS' + Ld\theta'' = 0, \tag{10}$$

$$\phi'' + Lnf\phi' + \frac{Nt}{Nb}\theta'' = 0, \tag{11}$$

subject to the boundary conditions

$$\begin{aligned} &f = 0, \qquad f' = 1, \qquad \theta = 1, \qquad S = 1, \qquad \phi = 1 \quad \text{at } \eta = 0, \\ &f' \to 0, \qquad \theta \to 0, \qquad S \to 0, \qquad \phi \to 0 \quad \text{as } \eta \to \infty. \end{aligned} \tag{12}$$

The parameters in equations (8)-(11) are the magnetic number M, the Prandtl number Pr, the Lewis number Le, the Brownian motion parameter Nb, the thermophoresis parameter Nt, the nanofluid Lewis number Ln, the modified Dufour parameter Nd and the Dufour-solutal Lewis number Ld. These parameters are defined as

$$\begin{aligned} &M = \frac{\sigma B_0^2}{\rho_f a}, \qquad Pr = \frac{\nu}{\alpha}, \qquad Le = \frac{\alpha}{D_S}, \qquad Nb = \frac{\tau D_B(\hat{\phi}_w - \hat{\phi}_\infty)}{\nu}, \\ &Nt = \frac{\tau D_T(T_w - T_\infty)}{T_\infty \nu}, \qquad Ln = \frac{\nu}{D_B}, \\ &Nd = \frac{D_{TC}(C_w - C_\infty)}{\alpha(T_w - T_\infty)}, \qquad Ld = \frac{D_{CT}(T_w - T_\infty)}{D_S(C_w - C_\infty)}. \end{aligned}$$

The parameters of engineering interest in heat and mass transport problems are the local Nusselt number Nu_x, the Sherwood number Sh_x and the nanofluid Sherwood number

$Sh_{x,n}$. These parameters characterise the wall heat, the regular and nano mass transfer rates, respectively, and are defined by

$$Nu_x = \frac{-x}{T_w - T_\infty}\left(\frac{\partial T}{\partial y}\right)\Big|_{y=0} = -Re_x^{\frac{1}{2}}\theta'(0),$$

$$Shr_x = \frac{-x}{C_w - C_\infty}\left(\frac{\partial C}{\partial y}\right)\Big|_{y=0} = -Re_x^{\frac{1}{2}}S'(0),$$

$$Sh_{x,n} = \frac{-x}{\hat{\phi}_w - \hat{\phi}_\infty}\left(\frac{\partial \hat{\phi}}{\partial y}\right)\Big|_{y=0} = -Re_x^{\frac{1}{2}}\phi'(0).$$

Following Khan and Aziz [29], the physical parameters of interest are the reduced Nusselt Nur, the Sherwood number $\hat{Sh}$ and the reduced Sherwood Shr defined as

$$Nur = Nu_x/Re_x^{\frac{1}{2}}, \qquad Shr = Sh_{x,n}/Re_x^{\frac{1}{2}} \quad \text{and} \quad Sh = \widehat{Sh}_x/Re_x^{\frac{1}{2}}.$$

3 Method of solution

The system of equations (8)-(11) together with the boundary conditions (12) were solved using the successive linearisation method (SLM) (see [25, 26, 30]). The unknown functions $f(\eta)$, $\theta(\eta)$, $S(\eta)$ and $\phi(\eta)$ are expanded as

$$\left.\begin{array}{ll} f(\eta) = f_i(\eta) + \sum_{m=0}^{i-1} F_m(\eta), & \theta(\eta) = \theta_i(\eta) + \sum_{m=0}^{i-1} \Theta_m(\eta), \\ S(\eta) = S_i(\eta) + \sum_{m=0}^{i-1} \widetilde{S}_m(\eta), & \phi(\eta) = \phi_i(\eta) + \sum_{m=0}^{i-1} \Phi_m(\eta), \end{array}\right\} \tag{13}$$

where f_i, θ_i, S_i and ϕ_i are unknown and F_m, Θ_m, $\widetilde{S}_m$ and Φ_m ($m \geq 1$) are successive approximations that are obtained by recursively solving the linear forms of the equation system that results from substituting (13) into equations (8)-(11). In particular, the linearised equations to be solved are

$$F_i''' + a_{1,i-1}F_i'' + a_{2,i-1}F_i' + a_{3,i-1}F_i = \mathbf{r}_{1,i-1}, \tag{14}$$

$$\Theta_i'' + b_{1,i-1}\Theta_i' + b_{2,i-1}F_i + b_{3,i-1}\widetilde{S}_i'' + b_{4,i-1}\Phi_i' = \mathbf{r}_{2,i-1}, \tag{15}$$

$$\widetilde{S}_i'' + c_{1,i-1}\widetilde{S}_i' + c_{2,i-1}F_i + c_{3,i-1}\Theta_i'' = \mathbf{r}_{3,i-1}, \tag{16}$$

$$\Phi_i'' + d_{1,i-1}\Phi_i' + d_{2,i-1}F_i + d_{3,i-1}\Theta_i'' = \mathbf{r}_{4,i-1}, \tag{17}$$

subject to the boundary conditions

$$F_i(0) = F_i'(0) = F_i'(\infty) = \Theta_i(0) = \Theta_i(\infty) = \widetilde{S}_i(0) = \widetilde{S}_i(\infty) = \Phi_i(0) = \Phi_i(\infty) = 0, \tag{18}$$

where coefficient parameters $a_{k,i-1}$, $b_{k,i-1}$, $c_{k,i-1}$, $d_{k,i-1}$ ($k = 1, \ldots, 4$) and $r_{j,i-1}$ ($j = 1, \ldots, 4$) are known constants. The initial guesses $F_0(\eta)$, $\Theta_0(\eta)$, $\widetilde{S}_0(\eta)$ and $\Phi_0(\eta)$ are chosen to satisfy the boundary conditions

$$\left.\begin{array}{llllll} F_0(\eta) = 0, & F_0'(\eta) = 1, & \Theta_0(\eta) = 1, & \tilde{S}_0(\eta) = 1, & \Phi_0(\eta) = 1 & \text{at } \eta = 0, \\ F_0'(\eta) \to 0, & \Theta_0(\eta) \to 0, & \tilde{S}_0(\eta) \to 0, & \Phi_0(\eta) \to 0 & \text{as } \eta \to \infty & \end{array}\right\} \tag{19}$$

and are chosen as

$$F_0(\eta) = 1 - e^{-\eta}, \qquad \Theta_0(\eta) = e^{-\eta}, \qquad \widetilde{S}_0 = e^{-\eta}, \qquad \Phi_0(\eta) = e^{-\eta}. \tag{20}$$

Starting from the initial guesses and iterating M_1 times, the functions $f(\eta)$, $\theta(\eta)$ and $\phi(\eta)$ are written as

$$\begin{aligned} f(\eta) &\approx \sum_{m=0}^{M_1} F_m(\eta), \qquad \theta(\eta) \approx \sum_{m=0}^{M_1} \Theta_m(\eta), \\ S(\eta) &\approx \sum_{m=0}^{M_1} \widetilde{S}_m(\eta), \qquad \Phi(\eta) \approx \sum_{m=0}^{M_1} \Phi_m(\eta), \end{aligned} \tag{21}$$

where M_1 is the order of the SLM approximation. Equations (14)-(17) are solved using the Chebyshev spectral collocation method. The method is based on the Chebyshev polynomials defined on the interval $[-1,1]$. We first transform the domain of solution $[0,\infty)$ into the domain $[-1,1]$ using the domain truncation technique where the problem is solved in the interval $[0,L]$ where L is a scaling parameter used to invoke the boundary condition at infinity. This is achieved by using the mapping

$$\frac{\eta}{L} = \frac{\xi + 1}{2}, \quad -1 \le \xi \le 1. \tag{22}$$

We discretise the domain $[-1,1]$ using the Gauss-Lobatto collocation points given by

$$\xi = \cos\frac{\pi j}{N}, \quad j = 0,1,2,\ldots,N, \tag{23}$$

where N is the number of collocation points used. The functions F_i, Θ_i, $\widetilde{S}_i$ and Φ_i for $i \ge 1$ are approximated at the collocation points as follows:

$$\left.\begin{aligned} F_i(\xi_j) &\approx \textstyle\sum_{k=0}^{N} F_i(\xi_k) T_k(\xi_j), \qquad \Theta_i(\xi_j) \approx \sum_{k=0}^{N} \Theta_i(\xi_k) T_k(\xi_j), \\ \widetilde{S}_i(\xi_j) &\approx \textstyle\sum_{k=0}^{N} \widetilde{S}_i(\xi_k) T_k(\xi_j), \qquad \Phi_i(\xi_j) \approx \sum_{k=0}^{N} \Phi_i(\xi_k) T_k(\xi_j), \end{aligned}\right\} \quad j = 0,1,\ldots,N, \tag{24}$$

where T_k is the kth Chebyshev polynomial given by

$$T_k(\xi) = \cos\bigl[k \cos^{-1}(\xi)\bigr]. \tag{25}$$

The derivatives of the variables evaluated at the collocation points $\xi = \xi_j$ are represented as

$$\left.\begin{aligned} \tfrac{d^r F_i}{d\eta^r} &= \textstyle\sum_{k=0}^{N} \mathbf{D}_{jk}^r F_i(\xi_k), \qquad \tfrac{d^r \Theta_i}{d\eta^r} = \sum_{k=0}^{N} \mathbf{D}_{jk}^r \Theta_i(\xi_k), \\ \tfrac{d^r \Theta_i}{d\eta^r} &= \textstyle\sum_{k=0}^{N} \mathbf{D}_{jk}^r \Theta_i(\xi_k), \qquad \tfrac{d^r \Phi_i}{d\eta^r} = \sum_{k=0}^{N} \mathbf{D}_{jk}^r \Phi_i(\xi_k), \end{aligned}\right\} \quad j = 0,1,\ldots,N, \tag{26}$$

where r is the order of differentiation and $\mathbf{D} = \frac{2}{L}\mathcal{D}$ with $\mathcal{D}$ being the Chebyshev spectral differentiation matrix (see, for example, [31–33]), whose entries are defined as

$$\left.\begin{aligned} &\mathcal{D}_{00} = \tfrac{2N^2+1}{6}, \\ &\mathcal{D}_{jk} = \tfrac{c_j}{c_k}\tfrac{(-1)^{j+k}}{\xi_j-\xi_k}, \quad j \neq k; j,k = 0,1,\ldots,N, \\ &\mathcal{D}_{kk} = -\tfrac{\xi_k}{2(1-\xi_k^2)}, \quad k = 1,2,\ldots,N-1, \\ &\mathcal{D}_{NN} = -\tfrac{2N^2+1}{6}. \end{aligned}\right\} \tag{27}$$

Substituting equations (22)-(26) into equations (14)-(17) leads to the matrix equation

$$\mathbf{A}_{i-1}\mathbf{X}_i = \mathbf{R}_{i-1}, \tag{28}$$

where $\mathbf{A}_{i-1}$ is a $(4N+4)\times(4N+4)$ square matrix and $\mathbf{X}_i$ and $\mathbf{R}_{i-1}$ are $(4N+4)\times 1$ column vectors defined by

$$\mathbf{A}_{i-1} = \begin{bmatrix} A_{11} & A_{12} & A_{13} & A_{14} \\ A_{21} & A_{22} & A_{23} & A_{24} \\ A_{31} & A_{32} & A_{33} & A_{34} \\ A_{41} & A_{42} & A_{43} & A_{44} \end{bmatrix}, \qquad \mathbf{X}_i = \begin{bmatrix} F_i \\ \Theta_i \\ \widetilde{S} \\ \Phi_i \end{bmatrix}, \qquad \mathbf{R}_{i-1} = \begin{bmatrix} \mathbf{r}_{1,i-1} \\ \mathbf{r}_{2,i-1} \\ \mathbf{r}_{3,i-1} \\ \mathbf{r}_{4,i-1} \end{bmatrix}. \tag{29}$$

The functions and parameters in equation (29) are

$$\begin{aligned} &F_i = \left[f_i(\xi_0), f_i(\xi_1), \ldots, f_i(\xi_{N-1}), f_i(\xi_N)\right]^T, \\ &\Theta_i = \left[\theta_i(\xi_0), \theta_i(\xi_1), \ldots, \theta_i(\xi_{N-1}), \theta_i(\xi_N)\right]^T, \\ &\widetilde{S}_i = \left[S_i(\xi_0), \theta_i(\xi_1), \ldots, S_i(\xi_{N-1}), S_i(\xi_N)\right]^T, \\ &\Phi_i = \left[\phi_i(\xi_0), \phi_i(\xi_1), \ldots, \phi_i(\xi_{N-1}), \phi_i(\xi_N)\right]^T, \\ &\mathbf{r}_{1,i-1} = \left[r_{1,i-1}(\xi_0), r_{1,i-1}(\xi_1), \ldots, r_{1,i-1}(\xi_{N-1}), r_{1,i-1}(\xi_N)\right]^T, \\ &\mathbf{r}_{2,i-1} = \left[r_{2,i-1}(\xi_0), r_{2,i-1}(\xi_1), \ldots, r_{2,i-1}(\xi_{N-1}), r_{2,i-1}(\xi_N)\right]^T, \\ &\mathbf{r}_{3,i-1} = \left[r_{3,i-1}(\xi_0), r_{3,i-1}(\xi_1), \ldots, r_{3,i-1}(\xi_{N-1}), r_{3,i-1}(\xi_N)\right]^T, \\ &\mathbf{r}_{4,i-1} = \left[r_{3,i-1}(\xi_0), r_{3,i-1}(\xi_1), \ldots, r_{3,i-1}(\xi_{N-1}), r_{3,i-1}(\xi_N)\right]^T, \\ &A_{11} = \mathbf{D}^3 + \mathbf{a}_{1,i-1}\mathbf{D}^2 + \mathbf{a}_{2,i-1}\mathbf{D} + \mathbf{a}_{3,i-1}\mathbf{I}, \qquad A_{12} = [\mathbf{0}], \qquad A_{13} = [\mathbf{0}], \qquad A_{14} = [\mathbf{0}], \\ &A_{21} = \mathbf{b}_{2,i-1}\mathbf{I}, \qquad A_{22} = \mathbf{D}^2 + \mathbf{b}_{1,i-1}\mathbf{D}, \qquad A_{23} = \mathbf{b}_{3,i-1}\mathbf{D}^2, \qquad A_{24} = \mathbf{b}_{4,i-1}\mathbf{D}, \\ &A_{31} = \mathbf{c}_{2,i-1}\mathbf{I}, \qquad A_{32} = \mathbf{c}_{3,i-1}\mathbf{D}^2, \qquad A_{33} = \mathbf{D}^2 + \mathbf{c}_{1,i-1}\mathbf{D}, \qquad A_{34} = [\mathbf{0}], \\ &A_{41} = \mathbf{d}_{2,i-1}\mathbf{I}, \qquad A_{42} = \mathbf{d}_{3,i-1}\mathbf{D}^2, \qquad A_{44} = [\mathbf{0}], \qquad A_{43} = \mathbf{D}^2 + \mathbf{d}_{1,i-1}\mathbf{D}. \end{aligned}$$

In the definitions above, T stands for transpose, $\mathbf{a}_{k,i-1}$ $(k = 1,\ldots,3)$, $\mathbf{b}_{k,i-1}$ $(k = 1,\ldots,4)$, $\mathbf{c}_{k,i-1}$ $(k = 1,\ldots,3)$, $\mathbf{d}_{k,i-1}$ $(k = 1,\ldots,3)$ and $\mathbf{r}_{k,i-1}$ $(k = 1,\ldots,4)$ are diagonal matrices of order $(N+1)\times(N+1)$, $\mathbf{I}$ is an identity matrix of order $(N+1)\times(N+1)$ and $[\mathbf{0}]$ is a zero matrix of order $(N+1)\times(N+1)$. The solution is obtained as

$$\mathbf{X}_i = \mathbf{A}_{i-1}^{-1}\mathbf{R}_{i-1}. \tag{30}$$

Table 1 Comparison of results for the reduced Nusselt number $-\theta(0)$ with $M = 0$, $Pr = 10$, $Le = 10$

Nb	*Nt*	$-\theta(0)$				
		Khan and Pop [15]	Present results			
			Ord 2	Ord 4	Ord 5	Ord 6
0.1	0.1	0.9524	0.954110803008	0.952376830835	0.952376830835	0.952376830835
	0.2	0.6932	0.696282777163	0.693174335745	0.693174335745	0.693174335745
	0.3	0.5201	0.523772737719	0.520079246363	0.520079246361	0.520079246361
	0.4	0.4026	0.406474865249	0.402579651548	0.402579651503	0.402579651503
	0.5	0.3211	0.325192006813	0.321057339674	0.321057339175	0.321057339175
0.2	0.1	0.5056	0.507610155261	0.505578818179	0.505578818179	0.505578818179
	0.2	0.3654	0.367853633248	0.365368345283	0.365368345283	0.365368345283
	0.3	0.2731	0.275387707176	0.273079280934	0.273079280931	0.273079280931
	0.4	0.2110	0.213054455507	0.210961536564	0.210961536512	0.210961536512
	0.5	0.1681	0.170080726148	0.168004798568	0.168004798105	0.168004798105
0.3	0.1	0.2522	0.253142109948	0.252145911886	0.252145911886	0.252145911886
	0.2	0.1816	0.182448890243	0.181611610633	0.181611610633	0.181611610633
	0.3	0.1355	0.136247585715	0.135548634738	0.135548634736	0.135548634736
	0.4	0.1046	0.105143130395	0.104494777320	0.104494777289	0.104494777289
	0.5	0.0833	0.083748729977	0.083300228592	0.083300228332	0.083300228332
0.4	0.1	0.1194	0.119563178994	0.119374160613	0.119374160613	0.119374160613
	0.2	0.0859	0.086351287057	0.085925168149	0.085925168149	0.085925168149
	0.3	0.0641	0.064969735925	0.064079763378	0.064079763377	0.064079763377
	0.4	0.0495	0.050308680850	0.049312783009	0.049312782995	0.049312782995
	0.5	0.0394	0.040068826105	0.039480432439	0.039480432335	0.039480432335
0.5	0.1	0.0543	0.055006822209	0.054252883744	0.054252883744	0.054252883744
	0.2	0.0390	0.041220738923	0.039039843265	0.039039843265	0.039039843265
	0.3	0.0291	0.032448207734	0.029136702982	0.029136702982	0.029136702982
	0.4	0.0225	0.025991804960	0.022499022345	0.022499022340	0.022499022340
	0.5	0.0179	0.020636326976	0.017899977204	0.017899977138	0.017899977138

4 Results and discussion

In this section we present solutions of equations (8)-(11) along with the boundary conditions (12) using the SLM iteration scheme. Tables 1 and 2 give a comparison between the present results and Khan and Pop [15] for the reduced Nusselt and Sherwood numbers respectively. There is a good agreement between the two sets of results with the SLM having converged at the fourth order up to eleven decimal places. The velocity components $f(\eta)$ and $f'(\eta)$ are plotted in Figures 1(a) and 1(b) for different values of the magnetic field parameter M. As is now well known, the velocity decreases with increases in the magnetic field parameter due to an increase in the Lorentz drag force that opposes the fluid motion.

Figures 2(a) and 2(b) show the effect of the thermophoresis parameter on the temperature and mass volume fraction profiles. The thermophoretic force generated by the temperature gradient creates a fast flow away from the stretching surface. In this way more fluid is heated away from the surface, and consequently, as Nt increases, the temperature within the boundary layer increases. The fast flow from the stretching sheet carries with it nanoparticles leading to an increase in the mass volume fraction boundary layer thickness.

Figures 3(a) and 3(b) show the effect of the Lewis number Le, and the Dufour-solutal Lewis number Ld on the species concentration in the boundary layer. The concentration profiles significantly contract as the Lewis number increases. The effect of the random motion of the nanoparticles suspended in the fluid on the temperature and nanoparticle volume fraction is shown in Figures 4(a) and 4(b). As expected, the increased Brownian motion of the nanoparticles carries with it heat and the thickness of the thermal bound-

Table 2 Comparison of results for the reduced Sherwood number $-\phi(0)$ with $M = 0$, $Pr = 10$, $Le = 10$

Nb	*Nt*	$-\phi(0)$				
		Khan and Pop [15]	Present results			
			Ord 2	Ord 4	Ord 5	Ord 6
0.1	0.1	2.1294	2.127980595220	2.129393826738	2.129393826738	2.129393826738
	0.2	2.2740	2.269600795082	2.274021155237	2.274021155237	2.274021155237
	0.3	2.5286	2.522442790300	2.528634341968	2.528634341973	2.528634341973
	0.4	2.7952	2.789547614977	2.795197381386	2.795197381518	2.795197381518
	0.5	3.0351	3.031692110921	3.035086541257	3.035086542806	3.035086542806
0.2	0.1	2.3819	2.381135534775	2.381870765082	2.381870765082	2.381870765082
	0.2	2.5152	2.513872542870	2.515221791508	2.515221791508	2.515221791508
	0.3	2.6555	2.654621334344	2.655461783297	2.655461783300	2.655461783300
	0.4	2.7818	2.782448136707	2.781787213285	2.781787213347	2.781787213347
	0.5	2.8883	2.891077315907	2.888289878800	2.888289879328	2.888289879328
0.3	0.1	2.4100	2.409868561539	2.410018897249	2.410018897249	2.410018897249
	0.2	2.5150	2.515064990923	2.514994504216	2.514994504216	2.514994504216
	0.3	2.6088	2.609550527921	2.608824244439	2.608824244440	2.608824244440
	0.4	2.6876	2.689475214512	2.687604301826	2.687604301841	2.687604301841
	0.5	2.7519	2.755453212842	2.751842541500	2.751842541544	2.751842541544
0.4	0.1	2.3997	2.399691610597	2.399650250624	2.399650250624	2.399650250624
	0.2	2.4807	2.480840530130	2.480738445269	2.480738445269	2.480738445269
	0.3	2.5486	2.548758207066	2.548611975329	2.548611975329	2.548611975329
	0.4	2.6038	2.604477947716	2.603832566300	2.603832566297	2.603832566297
	0.5	2.6483	2.650218941812	2.648243871234	2.648243871122	2.648243871122
0.5	0.1	2.3836	2.383468564586	2.383571426509	2.383571426509	2.383571426509
	0.2	2.4468	2.446168708773	2.446806984545	2.446806984545	2.446806984545
	0.3	2.4984	2.497045285759	2.498378497565	2.498378497565	2.498378497565
	0.4	2.5399	2.538409035362	2.539849811783	2.539849811777	2.539849811777
	0.5	2.5731	2.572599764241	2.573109330795	2.573109330658	2.573109330658

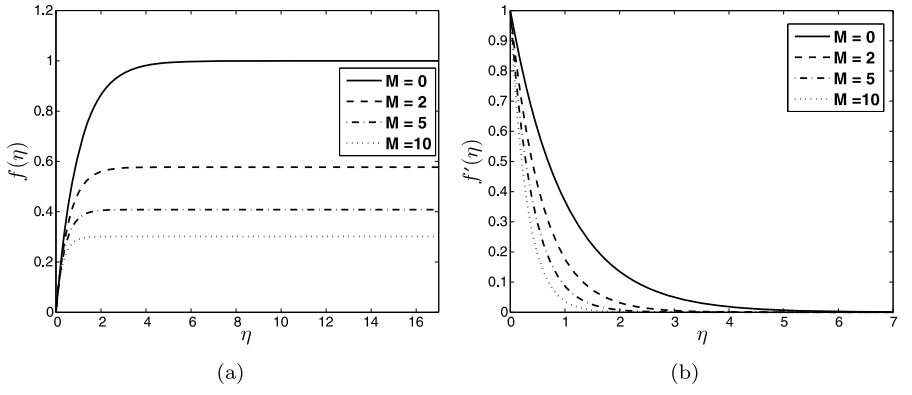

Figure 1 Effect of the magnetic field M on the velocity components (a) $f(\eta)$ and (b) $f'(\eta)$.

ary layer increases. The Brownian motion of the nanoparticles increases thermal transport which is an important mechanism for the enhancement of thermal conductivity of nanofluids. However, we note that increasing the Brownian motion parameter leads to a clustering of the nanoparticles near the stretching sheet. An increase in the Brownian motion of the nanoparticles leads to a decrease in the mass volume fraction profiles.

Figures 5(a) and 5(b) show the temperature profiles for several values of the Prandtl number Pr and mass volume fraction profile for several values of the modified Dufour

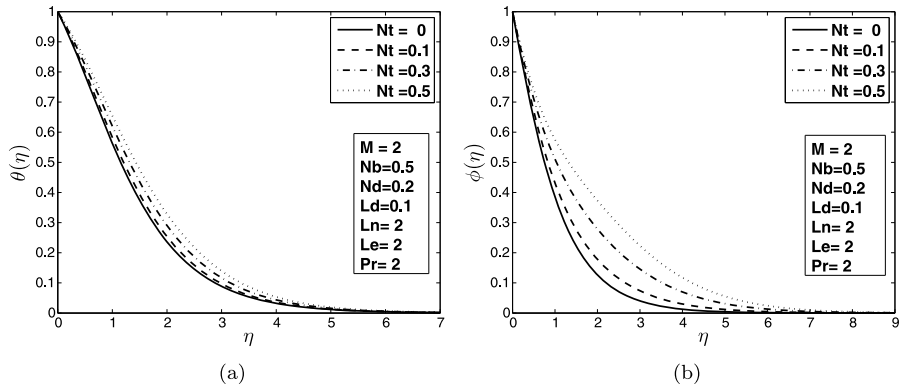

Figure 2 Effect of the thermophoresis parameter *Nt* on the temperature θ and nanoparticle ϕ profiles.

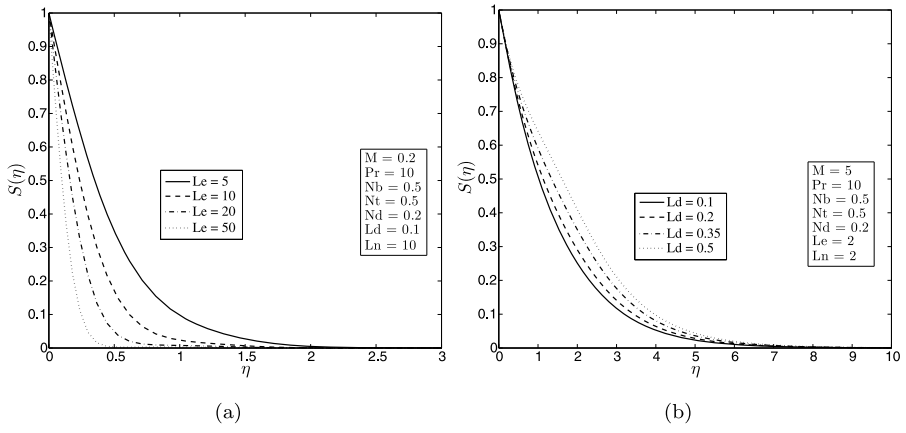

Figure 3 Effect of the Lewis number *Le* and the Dufour-solutal Lewis number *Ld* on concentration profiles.

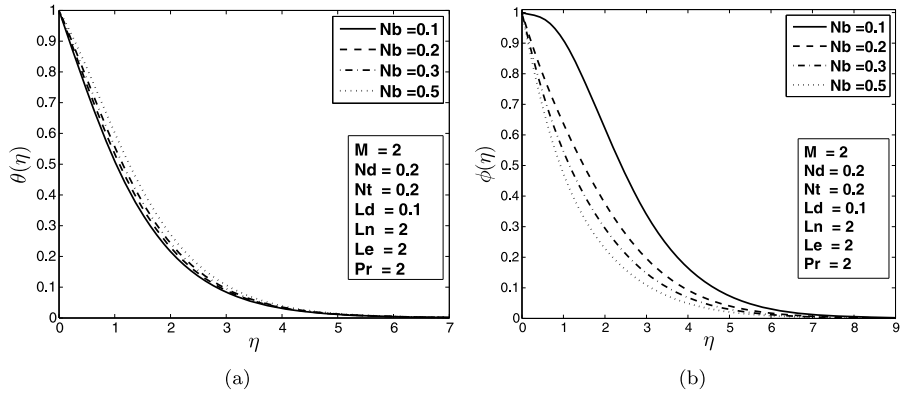

Figure 4 Effect of the Brownian motion parameter *Nb* on the temperature and nanoparticle volume fraction profiles.

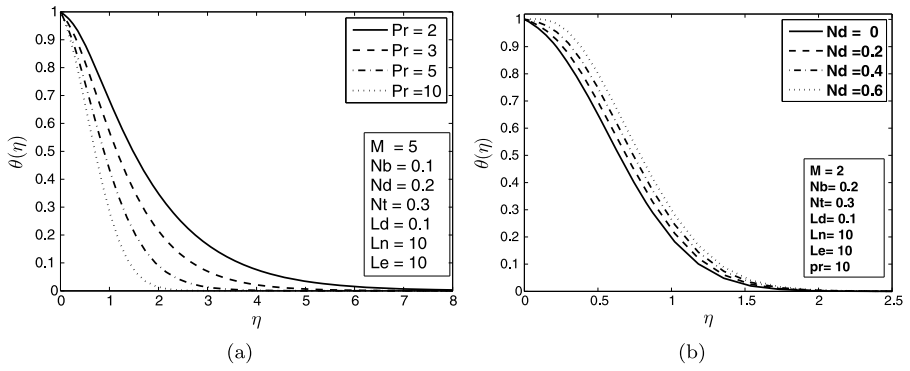

Figure 5 Effect of *Pr* and *Nd* on the temperature θ, profiles respectively.

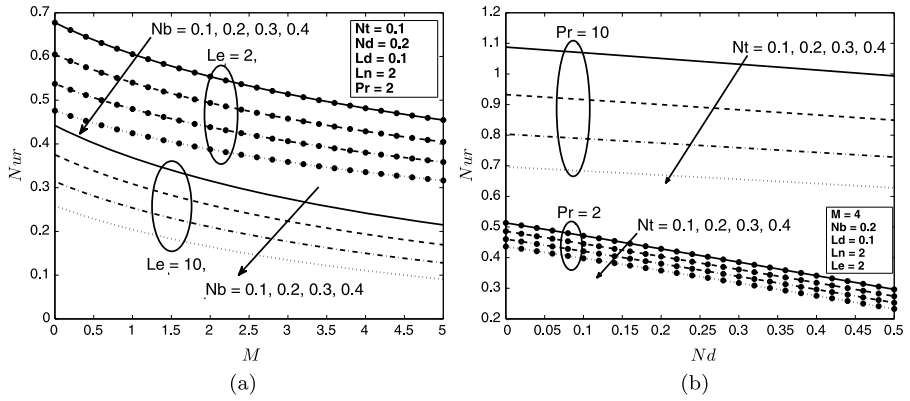

Figure 6 Effect of *Nt*, *Le*, *Pr*, *Nd* and *M* on the heat transfer coefficient *Nur*.

number *Nd*. The temperature profiles decrease as the Prandtl number increases since, for high Prandtl numbers, the flow is governed by momentum and viscous diffusion rather than thermal diffusion. On the other hand, the thickness of the mass volume fraction boundary layer increases with an increase in *Nd*.

Figures 6(a) and 6(b) show the effects of the thermophoresis parameter *Nt*, the Lewis number *Le*, the magnetic field parameter *M*, the Prandtl number *Pr* and the modified Dufour number *Nd* on the wall heat and mass fraction transfer rates. It can be seen that the thermal boundary layer thickness increases when the thermophoresis parameter *Nt* increases, thus decreasing the reduced Nusselt number. However, increasing the Lewis number *Le* leads to a decrease in the reduced Nusselt number. On the other hand, the results show that the reduced Nusselt number increases with increasing Prandtl numbers. Increasing both the magnetic field parameter *M* and the modified Dufour parameter *Nd* leads to an increase in the thermal boundary layer thickness, thus reducing the Nusselt number.

Figures 7(a) and 7(b) show the effects of the Dufour-solutal Lewis number *Ld* and the nanofluid Lewis number *Ln* on the reduced Nusselt number *Nur* as the Brownian motion parameter *Nb* increases. We note a decrease in the reduced Nusselt number when *Ln* increases, and an increase in the reduced Nusselt number when *Ld* increases.

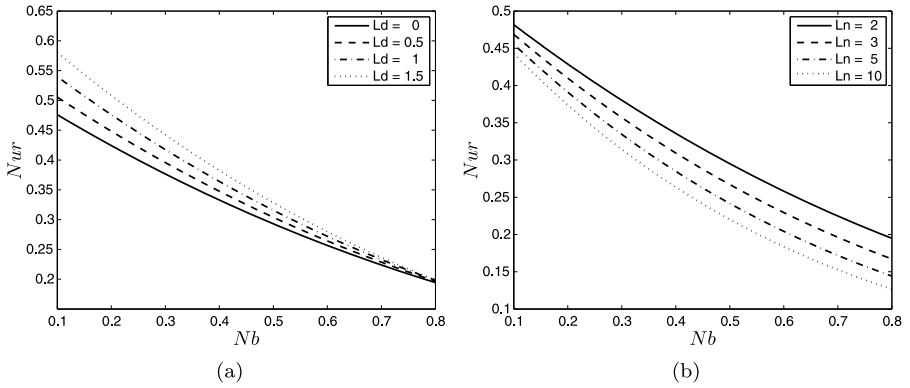

Figure 7 Effect of the Dufour-solutal Lewis number *Ld* and the nanofluid Lewis number *Ln* on the reduced Nusselt number *Nur*.

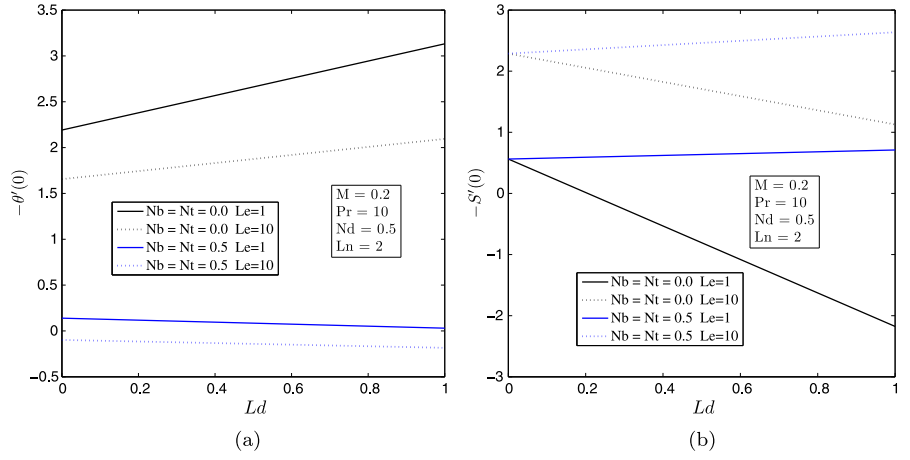

Figure 8 Effect of the Lewis number *Le*, the thermophoresis parameter *Nt* and the Brownian motion parameter *Nb* on (a) the reduced Nusselt number $-\theta'(0)$ and (b) the local Sherwood number $-S'(0)$.

Figures 8(a) and 8(b) show the graphs of $-\theta'(0)$ and $S'(0)$ plotted against the Dufour-solutal Lewis number Ld for different values of the parameters Nt, Nb and Le. We observe that $-\theta'(0)$ increases in the absence of the Brownian motion and the thermophoresis parameter while $-\theta'(0)$ decreases in the presence of Brownian motion and thermophoresis parameters. An increase in $-S'(0)$ is observed in the presence of both the Brownian motion and the thermophoresis parameter. Figures 9(a) and 9(b) show the effect of increasing Nt and Nb respectively on the reduced Sherwood number $-\phi(0)$.

5 Conclusions

A numerical study of the magneto-nanofluid boundary layer flow over a stretching sheet was carried out. We determined the effects of various parameters on the fluid properties as well as on the heat, and the regular and nano mass transfer rates. We have shown that increasing the magnetic field parameter M tends to retard the fluid flow within the boundary layer. The effects of the Prandtl number, the Lewis number, the Brownian motion parameter, the thermophoresis parameter, the nanofluid Lewis number, the modified Dufour parameter and the Dufour-solutal Lewis number on the heat, regular and nano

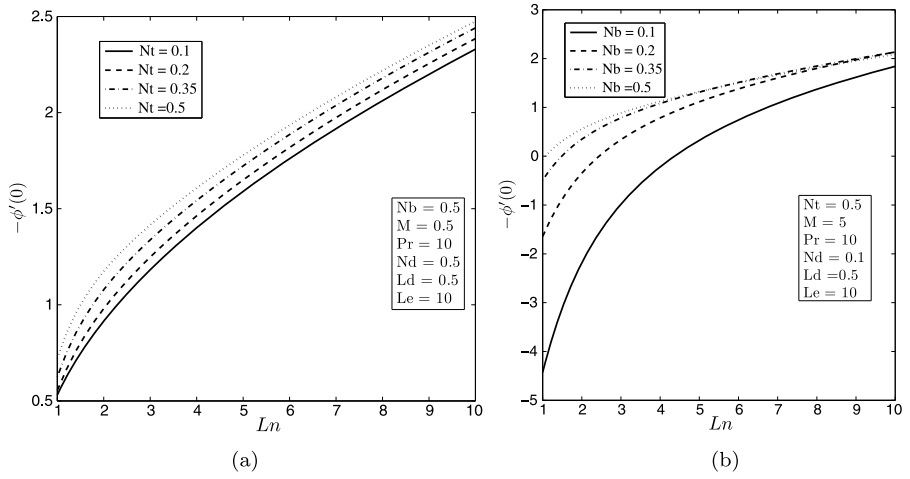

Figure 9 Effect of the nanofluid Lewis number *Ln*, the thermophoresis parameter *Nt* and the Brownian motion parameter *Nb* on the nanofluid Sherwood number $-\phi'(0)$.

mass transfer coefficients and fluid flow characteristics have been studied. We have shown *inter alia* that:

- the thermal boundary layer thickness increases with the thermophoresis parameter;
- increasing the Lewis number reduces the heat transfer coefficient;
- the heat transfer coefficient increases in the absence of the Brownian motion and the thermophoresis parameter and decreases in the presence of Brownian motion and thermophoresis parameters.

Competing interests
The authors declare that they have no competing interests.

Authors' contributions
The work including proofreading was done by all the authors.

Acknowledgements
The authors wish to thank the University of KwaZulu-Natal for financial support.

Received: 23 November 2012 Accepted: 7 May 2013 Published: 24 May 2013

References

1. Choi, SUS: Enhancing thermal conductivity of fluid with nanoparticles. In: Developments and Applications of Non-Newtonian Flows, vol. 23, pp. 99-105. FED, New York (1995)
2. Kakac, S, Pramuanjaroenkij, A: Review of convective heat transfer enhancement with nanofluid. Int. J. Heat Mass Transf. **52**, 3187-3196 (2009)
3. Choi, SUS, Zhang, ZG, Yu, W, Lockwood, FE, Grulke, EA: Anomalously thermal conductivity enhancement in nanotube suspensions. Appl. Phys. Lett. **79**, 2252-2254 (2001)
4. Masuda, H, Ebata, A, Teramae, K, Hishinuma, N: Alteration of thermal conductivity and viscosity of liquid by dispersing ultra-fine particles. Netsu Bussei **7**, 227-233 (1993)
5. Eapen, J, Rusconi, R, Piazza, R, Yip, S: The classical nature of thermal conduction in nanofluids. J. Heat Transf. **132**, 102402 (2010)
6. Fan, J, Wang, L: Effective thermal conductivity of nanofluids: the effects of microstructure. J. Phys. D, Appl. Phys. **43**, 165501 (2010)
7. Nield, DA, Kuznetsov, AV: The Cheng-Minkowycz problem for natural convective boundary-layer flow over a porous medium saturated by a nanofluid. Int. J. Heat Mass Transf. **52**, 5792-5795 (2010)
8. Nield, DA, Kuznetsov, AV: Thermal instability in a porous medium layer saturated by a nanofluid: Brinkman model. Transp. Porous Media **81**, 409-422 (2010)
9. Aziz, A, Khan, WA, Pop, I: Free convection boundary layer flow past a horizontal flat plate embedded in porous medium filled by nanofluid containing gyrotactic microorganisms. Int. J. Therm. Sci. **56**, 48-57 (2012)
10. Cheng, C-Y: Free convection boundary layer flow over a horizontal cylinder of elliptic cross section in porus media saturated by a nanofluid. Int. Commun. Heat Mass Transf. **39**, 931-936 (2012)

11. Chamkha, A, Gorla, RSR, Ghodeswar, K: Non-similar solution for natural convective boundary layer flow over a sphere embedded in a porous medium saturated with a nanofluid. Transp. Porous Media **86**, 13-22 (2011)
12. Altan, T, Oh, S, Gegel, H: Metal Forming Fundamentals and Applications. Am. Soc. Metals, Metals Park (1979)
13. Fisher, EG: Extrusion of Plastics. Wiley, New York (1976)
14. Tidmore, Z, Klein, I: Engineering Principles of Plasticating Extrusion. Polymer Science and Engineering Series. Van Norstrand, New York (1970)
15. Khan, WA, Pop, I: Boundary layer flow of a nanofluid past a stretching sheet. Int. J. Heat Mass Transf. **53**, 2477-2483 (2010)
16. Makinde, OD, Aziz, A: Boundary layer flow of a nanofluid past a stretching sheet with a convective boundary condition. Int. J. Therm. Sci. **50**, 1326-1332 (2011)
17. Narayana, M, Sibanda, P: Laminar flow of a nanoliquid film over an unsteady stretching sheet. Int. J. Heat Mass Transf. **55**, 7552-7560 (2012)
18. Kameswaran, PK, Narayana, N, Sibanda, P, Murthy, PVSN: Hydromagnetic nanofluid flow due to a stretching or shrinking sheet with viscous dissipation and chemical reaction effects. Int. J. Heat Mass Transf. **55**, 7587-7595 (2012)
19. Shima, PD, Philip, J, Raj, B: Magnetically controllable nanofluid with tunable thermal conductivity and viscosity. Appl. Phys. Lett. **95**, 133112 (2009)
20. Ganguly, R, Sen, S, Puri, IK: Heat transfer augmentation using a magnetic fluid under the influence of a line dipole. J. Magn. Magn. Mater. **271**, 63-73 (2004)
21. Bachok, N, Ishak, A, Pop, I: Unsteady boundary-layer flow and heat transfer of a nanofluid over a permeable stretching/shrinking sheet. Int. J. Heat Mass Transf. **55**, 2102-2109 (2012)
22. Hamad, MAA, Ferdows, M: Similarity solutions to viscous flow and heat transfer of nanofluid over nonlinearly stretching sheet. Appl. Math. Mech. **33**, 923-930 (2012)
23. Makukula, ZG, Motsa, SS, Sibanda, P: On a new solution for the viscoelastic squeezing flow between two parallel plates. J. Adv. Res. Appl. Math. **2**, 31-38 (2010)
24. Awad, FG, Sibanda, P, Motsa, SS, Makinde, OD: Convection from an inverted cone in a porous medium with cross-diffusion effects. Comput. Math. Appl. **61**, 1431-1441 (2011)
25. Makukula, ZG, Sibanda, P, Motsa, SS: A novel numerical technique for two-dimensional laminar flow between two moving porous walls. Math. Probl. Eng. **2010**, Article ID 528956 (2010). doi:10.1155/2010/528956
26. Makukula, ZG, Motsa, SS, Sibanda, P: A novel numerical technique for two-dimensional laminar flow between two moving porous walls. Math. Probl. Eng. **2010**, Article ID 528956 (2010). doi:10.1155/2010/528956
27. Awad, FG, Sibanda, P, Narayana, M, Motsa, SS: Convection from a semi-finite plate in a fluid saturated porous medium with cross-diffusion and radiative heat transfer. Int. J. Phys. Sci. **6**, 4910-4923 (2011)
28. Motsa, SS, Sibanda, P, Shateyi, S: On a new quasi-linearization method for systems of nonlinear boundary value problems. Math. Methods Appl. Sci. **34**, 1406-1413 (2011)
29. Khan, WA, Aziz, A: Double-diffusive natural convective boundary layer flow in a porous medium saturated with a nanofluid over a vertical plate: prescribed surface heat, solute and nanoparticle fluxes. Int. J. Therm. Sci. **50**, 2154-2160 (2011)
30. Shateyi, S, Motsa, SS: Variable viscosity on magnetohydrodynamic fluid flow and heat transfer over an unsteady stretching surface with hall effect. Bound. Value Probl. **2010**, Article ID 257568 (2010). doi:10.1155/2010/257568
31. Canuto, C, Hussaini, MY, Quarteroni, A, Zang, TA: Spectral Methods in Fluid Dynamics. Springer, Berlin (1988)
32. Don, WS, Solomonoff, A: Accuracy and speed in computing the Chebyshev collocation derivative. SIAM J. Sci. Comput. **16**, 1253-1268 (1995)
33. Trefethen, LN: Spectral Methods in MATLAB. SIAM, Philadelphia (2000)

doi:10.1186/1687-2770-2013-136
Cite this article as: Awad et al.: Thermodiffusion effects on magneto-nanofluid flow over a stretching sheet. *Boundary Value Problems* 2013 **2013**:136.